# Selective resonance effect of the folded longitudinal phonon modes in the Raman spectra of SiC

T. Tomita,[1] S. Saito,[1] M. Baba,[1] M. Hundhausen,[2] T. Suemoto,[1] and S. Nakashima[3]
[1]*Institute for Solid State Physics, University of Tokyo, 5-1-5 Kashiwanoha, Kashiwa, Chiba 277-8581, Japan*
[2]*Institut für Technische Physik, University Erlangen-Nürnberg, Erwin-Rommel-Strasse 1, D-91058 Erlangen, Germany*
[3]*Department of Electrical and Electronic Engineering, Miyazaki University, 1-1 Gakuenkibanadai-nishi, Miyazaki 889-2192, Japan*
(Received 21 September 1999)

The resonant Raman spectra of 4H-SiC, 6H-SiC, and 15R-SiC were measured from visible excitation to ultraviolet excitation. A selective enhancement of the intensities of the folded longitudinal phonon modes relative to the nonfolded longitudinal optical phonon mode was found. To explain this, we used a bond-Raman-polarizability model with a one-dimensional lattice dynamics model. It uses bond Raman polarizabilities of three bond arrangements, which we assumed to have different excitation energy dependences. By using this model, we successfully reproduced the excitation energy dependence of the relative intensities of the folded longitudinal phonon modes. The bond Raman polarizabilities and force constants used in our calculations are common for all polytypes. We found that the bond Raman polarizabilities of the three bond arrangements had different resonance energies.

## I. INTRODUCTION

Silicon carbide (SiC) has recently been receiving more and more attention as a wide-band-gap semiconductor with possible applications as a high-temperature, high-power, high-speed, and radiation-resistant device material. One of its most specific features is the existence of many polytypes with various stacking orders of the Si-C bilayers. These structures can be regarded as natural superlattices (homosuperlattices). The electronic band structure and the phonon dispersion curves of SiC strongly depend on the kind of polytype due to the zone folding effect. This allows us to prepare various semiconductors having different electronic and phonon properties with the same composition, if we can intentionally control the polytype structures. This system is also of interest from the viewpoint of physics, because it provides good prototypical examples for investigating the microscopic contributions of electron-phonon interactions in wide-band-gap semiconductors.

The resonant Raman effect has long been known as a powerful tool for investigating the electron-phonon coupling. In artificial superlattices, such as the GaAs-AlAs system (heterosuperlattices), resonant Raman spectroscopy has been used to show the coupling of specific phonons with the electronic states of the constituent materials.[1] This kind of effect is basically understood in terms of electron-phonon coupling in each (bulklike) material. In contrast to this rather simple case, the resonant Raman effect in the SiC superlattices will provide a tool for studying more microscopic contributions of the electron-phonon interaction, because these superstructures are based on different orderings of the individual bonding of the constituent atoms. However, there are no experimental or theoretical reports on the resonant Raman effect in SiC to our knowledge. In this paper, we demonstrate the selective resonance effect of Raman intensity for various folded longitudinal phonons in SiC and propose a model based on the bond-polarizability concept in order to understand the experimental results.

The building units of the SiC crystals are double layers of Si and C atoms and the polytypes are constructed with different stacking orders of these double layers.[2] In 3C-SiC, Si-C double layers stack in the sequence $ABCABC\ldots$ in the [111] direction (which is called the $c$ axis), forming a zinc-blende structure. Here, $A$, $B$, and $C$ denote Si-C double layers with three different atomic sites within the plane. In 2H-SiC, they make an $ABAB\ldots$ stacking, corresponding to a wurtzite structure. All other polytypes consist of a mixture of cubic and hexagonal stacking sequences.

The stacking structure of 4H-SiC is shown in Fig. 1(a). In 4H-SiC, the Si-C bilayers stack in the sequence $ABCBABCB\ldots$. The unit cell of 4H-SiC is 4 times larger than that of 3C-SiC, and its Brillouin zone is one-fourth of that of 3C-SiC. As a result, the phonon dispersion curves in the $[00\xi]$ direction are folded, giving rise to new intersection points at the $\Gamma$ point as shown in Fig. 1(b).[3] The new phonon modes that appear at the $\Gamma$ point are termed FLO(2/4), FLA(4/4), and so on, where the number in the parentheses is the reduced wave vector of the corresponding phonon in the Brillouin zone of 3C-SiC. Here, FLO (FLA) stands for a folded longitudinal optic (acoustic) phonon. Each phonon mode splits into a doublet at the zone center, except for the mode corresponding to the zone edge phonon in 3C-SiC. The energy splittings of these doublets are typically a few wave numbers.

The relative intensity of the transverse modes (FTO and FTA) has been studied for visible excitation, and a bond-Raman-polarizability model was applied to reproduce the relative intensity of the FTO and FTA modes.[2,4,5] In contrast to the transverse modes, the relative intensities of the longitudinal modes have been interpreted only recently.[6] One of the difficulties in reproducing the observed intensities in the calculation lies in the very weak Raman intensity of the longitudinal mode in the off-resonance excitation condition. A more precise model was constructed to reproduce the weak features.

## II. EXPERIMENT

The Raman spectra were measured in a backscattering geometry using a triple-grating monochromator (SPEX

 

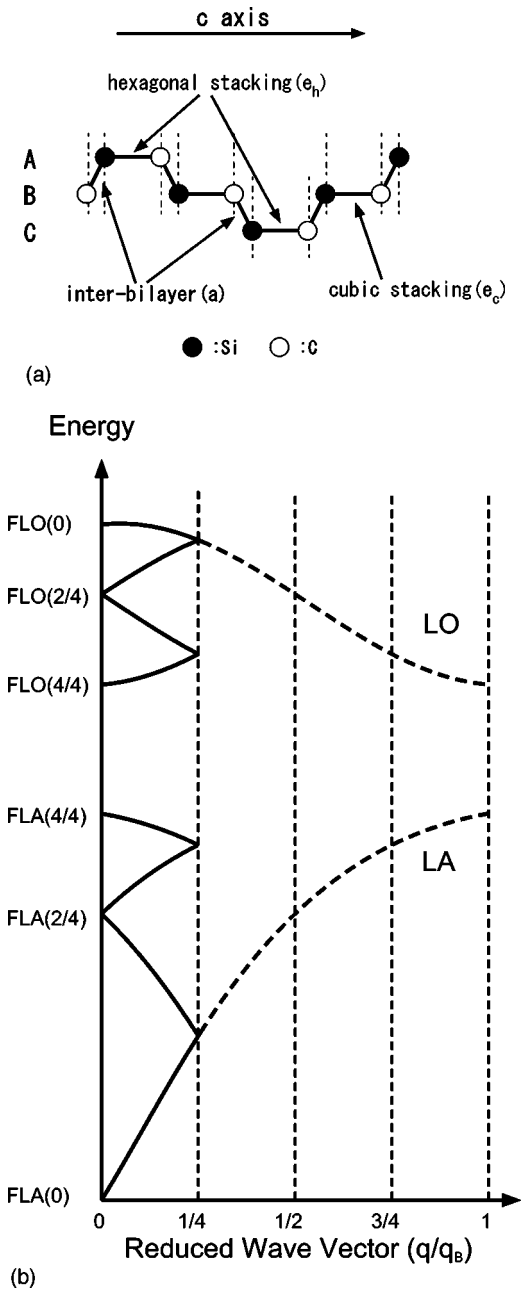


FIG. 1. (a) Stacking structure of 4H-SiC. Si-C double layers stack along the *c* axis. (b) Schematic dispersion curves of the longitudinal phonon modes in 4H-SiC.

1877) equipped with a cooled charge coupled device (CCD) camera. We took the spectra by using various lasers for excitation in the visible and ultraviolet regions at seven different wavelengths. The 457.9, 488.0, and 514.5 nm (2.71, 2.54, and 2.41 eV) lines were obtained from an Ar ion laser with a suitable interference filter or a prism to remove the plasma lines. For the 325 and 442 nm (3.81 and 2.81 eV) lines, we used a He-Cd laser. The power of the laser light ranged from 8 to 75 mW depending on the line. The second harmonic of a dye laser (Rh6G) synchronously pumped by a mode-locked yttrium aluminum garnet (YAG) laser was used at 302 nm (4.11 eV). The spectral width in this case was as large as 30 $cm^{-1}$ and the pulse width was a few picoseconds. The fourth harmonic of the *Q*-switched YAG laser was used as the 266 nm (4.66 eV) light source. This light was produced by passing the intracavity-frequency-doubled green light at 532 nm from a *Q*-switched YAG laser through a BBO crystal. The 266 nm light was separated from the 532 nm light by a prism and directed at the sample. The pulse width was 80 ns and the average power was about 24 mW. In that case, the spectral width of this laser was well below the resolution of the monochromator.

The SiC samples used in this study were flakelike crystals having (0001) as-grown surfaces produced by the Acheson process or a modified Lely process.[7] All samples were *n* type with impurity levels below $2\times10^{17}$ $cm^{-3}$.

Under resonant excitation conditions with a pulsed laser at 266 nm, the LO phonon readily couples with the plasmon and forms a coupled mode (LOPC) due to the high density of photoexcited carriers. In this case, the intensity of the FLO(0) mode is reduced. Therefore, we checked the excitation density dependence of the FLO(0) mode, and found that the effect of LOPC is negligible as long as we used a cylindrical lens ($f=100$ mm) for focusing the laser beam. For the other excitation sources with a wavelength above 266 nm, no peak shift or spectrum broadening of the FLO(0) mode was observed. Thus, the effect of photoexcited carriers can be neglected at all excitation wavelengths. The excitation density dependence of LOPC by photoexcited carriers will be discussed in detail in a separate paper.

The relative intensities of the folded longitudinal phonon modes are not affected by the geometrical configuration, because all the observable folded longitudinal phonon modes have $A_1$ symmetry.[8] Therefore, we did not analyze the polarization of the scattered light. The spectral response of the measurement system was checked by using a tungsten standard lamp, and the sensitivity was found to be practically flat within the wave number range of each Raman spectrum.

## III. RESULTS

The Raman spectra of 4H-SiC, 6H-SiC, and 15R-SiC are shown in Figs. 2(a), 3(a), and 4(a), respectively. Solid lines correspond to 266 nm excitation and dashed lines to 488 nm. The spectra were normalized to the FLO(0) mode. In our experimental conditions, the doublets of folded phonon modes could not be resolved.

The spectra show the enhancement of the intensity of the folded longitudinal phonon modes relative to the nonfolded FLO(0) mode for ultraviolet excitation. In 4H-SiC, the normalized intensities of the FLO(4/4) and FLA(4/4) modes are enhanced for ultraviolet excitation [see Fig. 2(a)]. In 6H-SiC, the FLO(4/6) and FLA(4/6) modes found for visible excitation are also enhanced for ultraviolet excitation [see Fig. 3(a)]. In 15R-SiC, the FLO(4/5), FLO(2/5), and FLA(4/5) modes are very weak for visible excitation, but they are strongly enhanced for ultraviolet excitation [see Fig. 4(a)].

The excitation energy dependence of the intensity of folded longitudinal phonon modes relative to the FLO(0) mode in 4H-SiC, 6H-SiC, and 15R-SiC is shown in Figs. 2(b), 3(b), and 4(b) by solid symbols, respectively. When the peak was not discernible, the noise level was plotted with an error bar to indicate the upper limit of the peak intensity.

In these figures, it can be seen that the normalized intensities of the folded longitudinal phonon modes are strongly enhanced for ultraviolet excitation. It is also worth noting

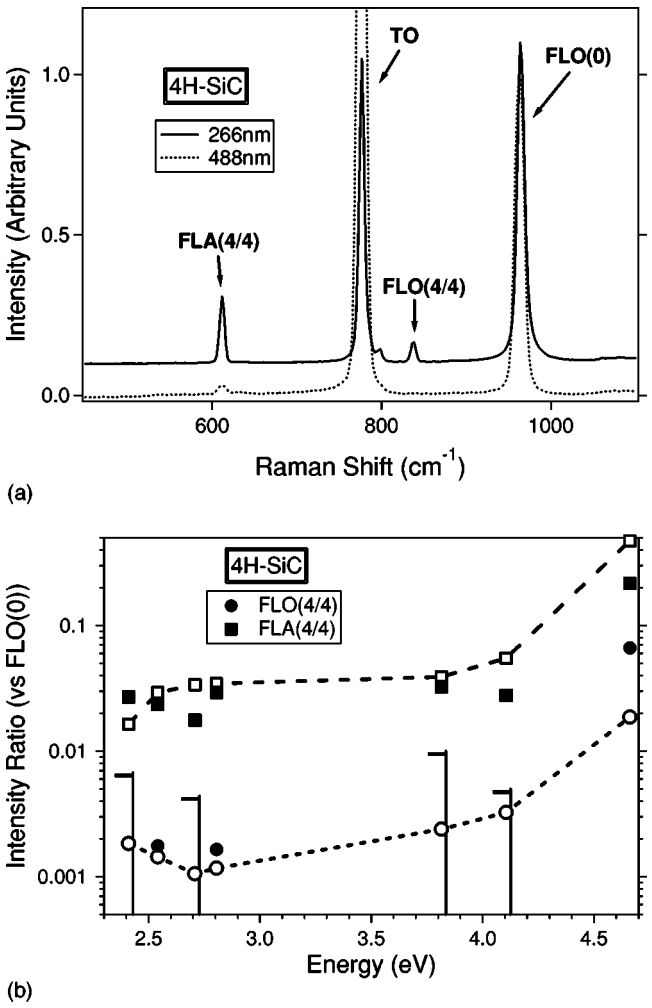


FIG. 2. (a) Raman spectra of 4H-SiC. Solid and dashed lines correspond to 266 nm and 488 nm excitation, respectively. The spectra are shifted by 0.1 along the ordinate for comparison. (b) Excitation energy dependence of the relative intensity of the folded longitudinal phonon modes for 4H-SiC. Solid symbols correspond to experimental data and open symbols with dashed lines correspond to calculated data. When the phonon peaks are not discernible against the noise, the noise level is shown by error bars.

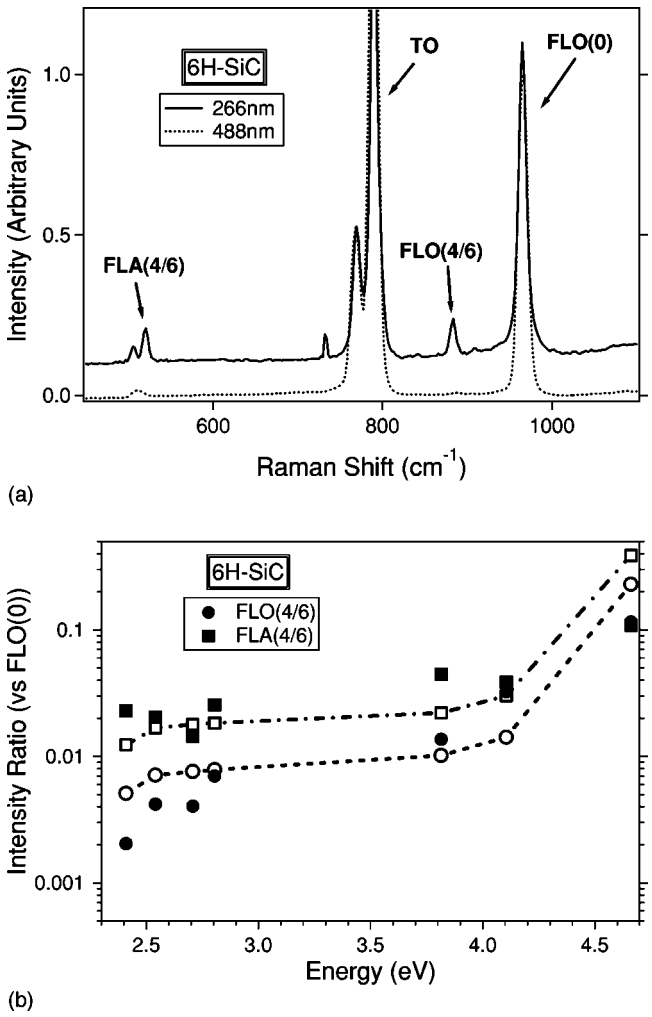


FIG. 3. (a) Raman spectra of 6H-SiC. Solid and dashed lines correspond to 266 nm and 488 nm excitation, respectively. The spectra are shifted by 0.1 along the ordinate for comparison. (b) Excitation energy dependence of the relative intensity of the folded longitudinal phonon modes for 6H-SiC. Notation is the same as that in Fig. 2(b).

that the relative intensities of these folded modes change. For example, the intensities of the FLO(4/6) and FLA(4/6) differ by a factor of about 10 at 2.4 eV, while they are almost the same at 4.6 eV.

TO-mode intensities significantly depend on excitation energy, as well. However, we will not discuss them further in this paper, because these modes are too closely spaced to be resolved due to the smaller dispersion of the transverse optical branch in SiC.

## IV. ANALYSIS

The selective resonance phenomena cannot easily be explained by transitions between electronic bands without considering the details of electron-phonon interactions. In order to understand the observed phenomena, we calculated the Raman intensity by using the bond-Raman-polarizability model.[9] In this calculation, we have to assume the model which can explain the large excitation energy dependence of the folded longitudinal phonon intensities in SiC. In Ref. 10, Clark and Mitchel discussed the Raman spectra of titanium tetraiodide by using the excitation-energy-dependent bond Raman polarizabilities. Although there is no report which assumed excitation-energy-dependent bond Raman polarizabilities in solids, as far as we know, this assumption is a natural extension of previous bond-Raman-polarizability calculations which correspond to fixed excitation energies. In the following, we calculate the Raman intensities assuming the excitation-energy-dependent bond Raman polarizabilities.

In advance, we had to determine the displacement of each phonon mode. The displacement of each atomic plane is calculated in a one-dimensional model, described by the equations of motion

$$M_j \frac{d^2 u_j^n}{dt^2} = \sum_{r,s} D_{j,j+s-mr}^r u_{j+s-mr}^{n+r}, \tag{1}$$

where

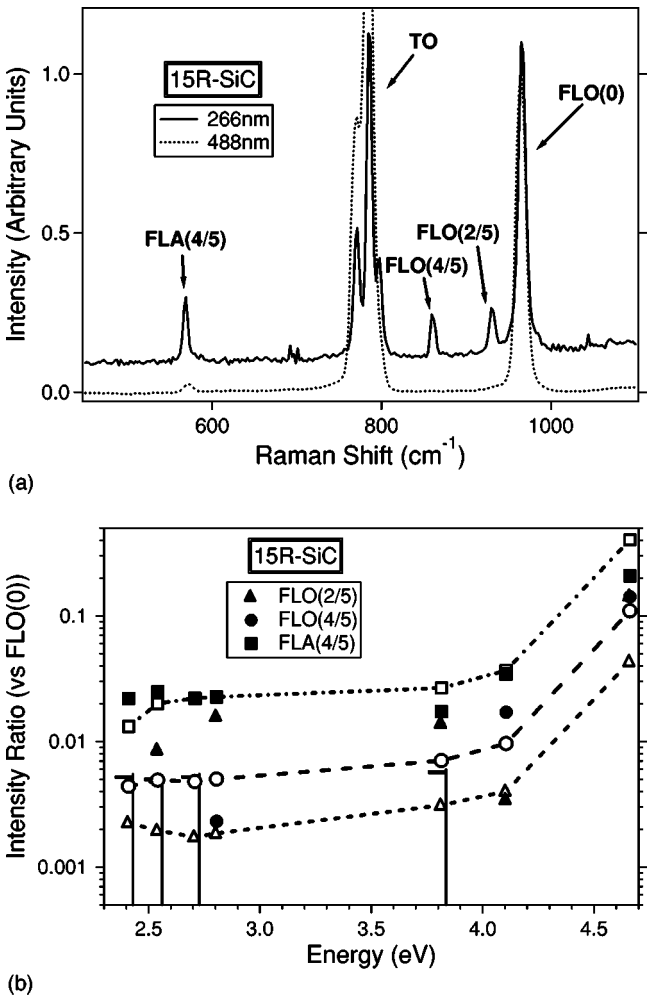


FIG. 4. (a) Raman spectra of 15R-SiC. Solid and dashed lines correspond to 266 nm and 488 nm excitation, respectively. The spectra are shifted by 0.1 along the ordinate for comparison. (b) Excitation energy dependence of relative intensity of the folded longitudinal phonon modes for 15R-SiC. Notation is the same as that in Fig. 2(b). Note that the solid circle and solid triangle fall on almost the same point at 4.66 eV.

$$r \equiv \left[ \frac{j+s}{m+1} \right]. \tag{2}$$

Here, $D^r_{j,j+s}$ denotes the interplanar force, $M$ the mass of each atom, $u$ the displacement of each atomic plane, $m$ the number of atoms in the unit cell, $n$ the label of unit cells, and $j$ the label of the atomic plane in the unit cell. $r$ equals 0, $\pm 1$, corresponding to the neighboring unit cells, and $s$ equals $0, \pm 1, \pm 2, \pm 3$, corresponding to the interplanar force up to the third neighbor. $[l]$ is Gauss' notation, which gives the largest integer that is smaller than or equal to $l$.

Here, we assume that $u^n_j$ is expressed as

$$u^n_j = u(j) \exp\{i(\omega t - q x_n)\}. \tag{3}$$

Here,

$$u(j) \equiv u^0_j, \tag{4}$$

where $\omega$ is the frequency, $q$ the $k$ transfer in light scattering, and $x_n$ the position of the $n$th unit cell.

TABLE I. Comparison between the observed and calculated energies of the folded longitudinal phonon modes for 488 nm excitation (Ref. 8). The upper branch of the doublet is indicated by + and the lower branch by −.

| Polytype | $q/q_B$ | Wave number ($cm^{-1}$) | | | |
|---|---|---|---|---|---|
| | | FLO | | FLA | |
| | | Expt. | Calc. | Expt. | Calc. |
| 4H | 0 | 964 | 965.9 | – | – |
| | 2/4 | – | – | – | – |
| | 4/4 | 838 | 837.1 | 610 | 614.2 |
| 6H | 0 | 965 | 966.3 | – | – |
| | 2/6 | – | – | – | – |
| | 4/6(+) | 889 | 888.7 | 514 | 510.7 |
| | 4/6(−) | | 883.5 | 504 | 504.0 |
| | 6/6 | – | – | – | – |
| 15R | 0 | 965 | 966.1 | – | – |
| | 2/5(+) | 938 | 937.5 | 337 | 335.5 |
| | 2/5(−) | 932 | 932.3 | 331 | 326.5 |
| | 4/5(+) | 860 | 860.1 | 577 | 573.8 |
| | 4/5(−) | | 857.9 | 569 | 569.4 |

Then, we obtain

$$-\omega^2 u(j) = \sum_k D'_{j,k} u(k), \tag{5}$$

where

$$D'_{j,k} \equiv \frac{1}{M_j} \sum_r D^r_{j,k} \exp(iqx_r). \tag{6}$$

Thus, the frequencies of folded phonon modes and the displacements of the atomic plane are obtained from the square root of eigenvalues and the eigenvectors of the matrix $D'_{j,k}$, respectively.

In this calculation, we considered force constants up to third-neighbor interactions by taking into account the stacking dependence of the force field. The nearest-neighbor force constants were distinguished into hexagonal, cubic, and interbilayer environments. The second-neighbor interactions have only two values, that is, silicon-silicon and carbon-carbon interactions. As the third-neighbor interactions, we assume three force constants depending on the stacking sequence. The same set of parameters was used to reproduce the energy of all the observed phonon modes in all polytypes simultaneously.

The experimentally observed frequencies of folded longitudinal phonon modes and the calculated frequencies are shown in Table I. In this table, the upper branch of a doublet is indicated by + and the lower branch by −. Note that the calculated energies reproduce the experimental ones within about 1%.

The calculated displacements of atoms are normalized according to

$$\hat{u} = N^{(\lambda)} u, \tag{7}$$

where

$$N^{(\lambda)}=\left\{\sum_j M_j\,|u^{(\lambda)}(j)|^2\right\}^{-1/2}. \tag{8}$$

The Raman polarizability of the $\lambda$th folded phonon mode can be expressed as

$$\alpha^{(\lambda)}=\sum_j d_j\{\hat{u}^{(\lambda)}(j)-\hat{u}^{(\lambda)}(j+1)\} \tag{9}$$

using the normalized displacement of each atom obtained from Eq. (7). Here, $d_j$ is the bond Raman polarizability, which we assumed differs for different stacking orders, as shown in Eq. (10) and Fig. 1(a):

$$d_j=\begin{cases} e_h & \text{(hexagonal stacking)},\\ e_c & \text{(cubic stacking)},\\ a & \text{(interbilayers)}. \end{cases} \tag{10}$$

These bond Raman polarizabilities are assumed to depend on excitation energy. In addition, we also assume different excitation energy dependences for each bond Raman polarizability given in Eq. (10).

The scattering intensity of the $\lambda$th folded phonon mode ($W^{(\lambda)}$) can be obtained from

$$W^{(\lambda)}=S\frac{n(\omega^{(\lambda)})+1}{\omega^{(\lambda)}}|\alpha^{(\lambda)}|^2, \tag{11}$$

where $n(\omega^{(\lambda)})$ is the Bose factor and $S$ is a constant independent of $\omega$.

In these calculations, the intensities of doublets of the folded phonon modes at the zone center are summed up, because we experimentally obtained only the intensity summations of doublets.

The values of the bond Raman polarizabilities ($e_c, e_h, a$) were adjusted to fit the experimental data for each excitation energy. It should be noted that the values of the bond Raman polarizability and force constants are the same for all three polytypes.

The calculated intensities of the folded phonon modes relative to FLO(0) mode are shown in Figs. 2(b), 3(b), and 4(b) by open symbols connected with dashed lines. As can be seen, the normalized intensity of the FLA(4/4) line is far higher than that of the FLO(4/4) line in 4H at all excitation energies [see Fig. 2(b)], while the intensities of the FLA(4/6) and FLO(4/6) lines are closer in 6H [see Fig. 3(b)]. This prominent difference between 4H and 6H in the experimentally observed resonant Raman spectra is well reproduced in our calculation. Furthermore, it is also possible to reproduce the increase in the normalized intensity for ultraviolet excitation. In 15R-SiC, the behavior of the FLA(4/5) and FLO(4/5) is well reproduced while the agreement of the FLO(2/5) is not satisfactory [see Fig. 4(b)].

In our calculation, the force constants are initially determined from fitting the dispersion curves of the longitudinal phonon modes, and then slightly tuning to reproduce the relative intensities of the folded phonon modes for 488 nm excitation. After these parameters have been fixed, the relative intensities of the folded longitudinal phonon modes are obtained using only two adjustable parameters ($e_c/a, e_h/a$).

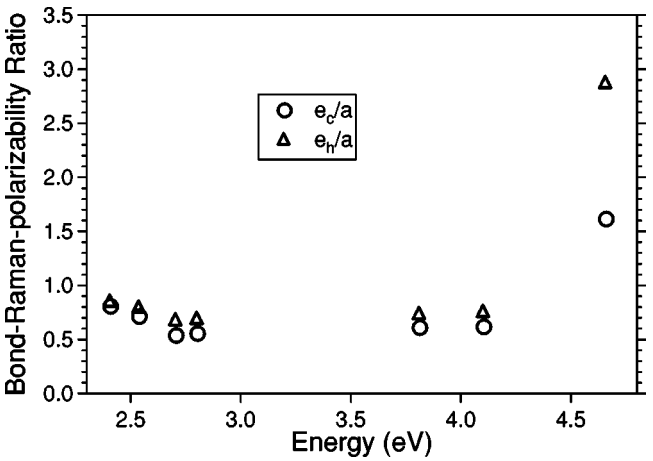


FIG. 5. Excitation energy dependence of the ratios of bond Raman polarizabilities, $e_c/a$ and $e_h/a$.

The ratios of the bond Raman polarizabilities thus determined for various energies are shown in Fig. 5. We can see that the values of $e_c$ and $e_h$ are enhanced in the ultraviolet region, relative to $a$. The values of $e_c$ and $e_h$ increase toward the direct band gap energy at the $\Gamma$ point, which lies around 5 eV in various SiC polytypes.[11] Furthermore, the difference between $e_c$ and $e_h$ also becomes larger in the ultraviolet region. We discuss the behavior of the bond Raman polarizabilities below.

In the nonfolded phonon mode, all bilayers oscillate in the same phase. On the other hand, for the folded phonon mode in a structure having a unit cell $n$ times larger than the zinc-blende structure, the phases of the neighboring bilayers differ by $2m\pi/n$ ($m$ is an integer and $|m|\leqslant n/2$), if the $k$ transfer in light scattering can be neglected. Then, in Eq. (9), the sum of the terms containing the displacements related to the interbilayer ($a$) bonds will be canceled out within the zinc-blende approximation which neglects the difference of force constants due to the stacking sequence. Actually, in this calculation, when the two bond Raman polarizabilities have the same value, i.e., $e_c=e_h$, all the calculated relative intensities of folded longitudinal phonon modes become practically zero, even if the effect of the $k$ transfer in the light scattering is included.[6] When the difference of $e_c$ and $e_h$ becomes larger, the normalized intensity of the folded phonon modes becomes larger. This means that the intensities of the folded longitudinal phonon modes relative to the FLO(0) mode are not sensitive to their magnitude but to the difference between $e_c$ and $e_h$. As a result, a similar intensity profile is obtained when $e_c$ and $e_h$ are exchanged.

The bond Raman polarizability originates in the bond charge localized between two neighboring atoms. In the simplest picture, this bond charge is a consequence of the additive overlap of two atomic orbitals forming a bonding state, while the subtractive overlap results in the antibonding state. The resonance energy of the bond Raman polarizability, which corresponds to the bonding to antibonding transition, will be large if the overlapping of the atomic orbitals is large.[12] In Ref. 13, it is shown that the bond length of the hexagonal stacking is slightly larger than that of the cubic stacking. As a result, the resonance energy will be lower in

the hexagonal stacking, because of the smaller overlap of the atomic orbitals. If we suppose that $e_c$ and $e_h$ have almost the same resonance profiles with the same intensity in ultraviolet region, then $e_h$ will be larger than $e_c$ at 4.66 eV. Judging from our data for excited energies ranging between 2.41 and 4.66 eV, the intensities of folded phonon modes do not have the tendency to vanish. Hence, we suppose that the values of $e_c$ and $e_h$ do not cross from 2.41 to 4.66 eV excitation, i.e., $e_h > e_c$ at all the excitation energies.

We obtain the resonance profiles of the relative bond Raman polarizabilities shown in Fig. 5. In the off-resonance conditions, the two bond Raman polarizabilities ($e_c$ and $e_h$) are expected to have values not very different, because only the third-neighbor arrangement differs between the bonds in the cubic and hexagonal environments. In near-resonance conditions, however, even a small difference in the resonance energies of $e_c$ and $e_h$ gives a large difference in the two bond Raman polarizabilities ($e_c$ and $e_h$), because of the large excitation energy dependence of $e_c$ and $e_h$.

## V. CONCLUSION

Selective enhancement in the relative Raman intensities of folded longitudinal phonon modes was found under ultraviolet excitation and the excitation energy dependence of the intensities of the folded longitudinal phonon modes relative to the FLO(0) mode was successfully interpreted in terms of a bond-Raman-polarizability model. In this model, we used only two Raman-polarizability parameters ($e_c/a, e_h/a$) to obtain reasonable agreement with the experimentally observed excitation energy dependence of the intensities of the folded longitudinal phonon modes for three polytypes simultaneously. The calculation shows that the Raman intensities of the folded longitudinal phonon modes are dominated by the difference between $e_c$ and $e_h$. Furthermore, we found that the bond Raman polarizabilities ($e_c$ and $e_h$) have different resonance energies.

Although our energy-dependent bond Raman polarizability model is rather intuitive, this model can reproduce the experimental data very well. Further theoretical study is required to understand the origin of the energy dependence in the bond Raman polarizabilities.

## ACKNOWLEDGMENTS

This work was partially supported by a Grant-In-Aid for Scientific Research (09450028) from the Japanese Ministry of Education, Science and Culture.

[1] A.K. Sood, J. Menéndez, M. Cardona, and K. Ploog, Phys. Rev. Lett. **54**, 2111 (1985).
[2] S. Nakashima and K. Tahara, Phys. Rev. B **40**, 6339 (1989).
[3] D.W. Feldman, James H. Parker, Jr., W.J. Choyke, and Lyle Patrick, Phys. Rev. **173**, 787 (1968).
[4] S. Nakashima, H. Katahama, Y. Nakakura, and A. Mitsuishi, Phys. Rev. B **33**, 5721 (1986).
[5] S. Nakashima and M. Hangyo, Solid State Commun. **80**, 21 (1991).
[6] S. Nakashima, H. Harima, T. Tomita, and T. Suemoto, Phys. Rev. B (to be published).
[7] J.A. Powell, D.J. Larkin, L.G. Matus, W.J. Choyke, J.L. Bradshaw, L. Henderson, M. Yoganathan, J. Yang, and P. Pirouz, Appl. Phys. Lett. **56**, 1442 (1990).
[8] S. Nakashima and H. Harima, Phys. Status Solidi A **162**, 39 (1997).
[9] S. Nakashima, H. Ohta, M. Hangyo, and B. Palosz, Philos. Mag. B **70**, 971 (1994).
[10] R.J.H. Clark and P.D. Mitchel, J. Am. Chem. Soc. **95**, 8300 (1973).
[11] G. Wellenhofer and U. Rössler, Phys. Status Solidi B **202**, 107 (1997).
[12] J.A. Van Vechten, Phys. Rev. B **7**, 1479 (1973).
[13] A. Bauer, J. Kräußlich, L. Dressler, P. Kuschnerus, J. Wolf, K. Goetz, P. Käckell, J. Furthmüller, and F. Bechstedt, Phys. Rev. B **57**, 2647 (1998).